The Added Value of Enhanced Depth Imaging-Optical Coherence Tomography in the Multimodal Imaging of Choroidal Nevi

O Benefício do *Enhanced Depth Imaging-Optical Coherence Tomography* na Avaliação Multimodal de Nevus Coroideus

Bruna Cunha [1], Pedro Gil [1], Catarina Mota [1], Diogo Hipólito-Fernandes [1], Ana Magriço [1]

[1] Ophthalmology Department, Centro Hospitalar e Universitário de Lisboa Central, Lisboa, Portugal

Recebido/Received: 2022-10-15 | **Aceite/Accepted:** 2023-04-16 | **Published online/Publicado online:** 2023-07-11 | **Publicado/Published:** 2023-12-29

DOI: https://doi.org/10.48560/rspo.28280

ABSTRACT

INTRODUCTION: To analyze the enhanced depth imaging (EDI) - optical coherence tomography (OCT) ability to identify, measure and classify choroidal nevi, and its correlation with high-risk features.

METHODS: Retrospective observational study of patients with choroidal nevi. Comprehensive eye examinations and multimodal imaging were performed for each nevus, including spectral domain EDI-OCT and B-scan ultrasonography (US). Main outcome measures were lesion thickness and features, EDI-OCT and US findings.

RESULTS: A total of 115 nevi (106 patients) were included. Five of the 115 nevi (4.4%) were considered suspicious lesions. Of the 114 nevi with reliable US, 83 (72.8%) were not identified, behaving as flat nevi. The mean largest basal dimension on US was 5.86 ± 2.19 mm (1.97-10.39 mm), and the mean maximal thickness was 1.37 ± 0.72 mm (0.45-2.95 mm). Sixty-two nevi had reliable EDI-OCT imaging. The mean maximum thickness on EDI-OCT was 404.93 ± 273.36 μm (139-1504 μm). The nevi maximum thickness measured in US was significantly different from the one measured by EDI-OCT (p=0.0011) for the same nevus, when both exams were reliable (US 1233.75 ± 549.57 μm; EDI-OCT 683.19 ± 343.80 μm). Thirty-eight of the 42 flat nevi on US that had an EDI-OCT performed over the lesion, were identified and measured by EDI-OCT, with a mean thickness lower than US detectability threshold. Eighteen of 62 nevi (29%) had elevation of the nevus surface and were classified as "elevated", type 4 on EDI-OCT. EDI-OCT type was positively associated with decrease in visual acuity (p=0.014) and the presence of intraretinal fluid or sub retinal fluid (SRF) on OCT (p=0.042). All the 5 suspicious lesions were associated with high-risk features of growth or transformation, such as decrease in visual acuity, thickness greater than 2 mm, largest basal dimension greater than 5 mm and SRF.

CONCLUSION: EDI-OCT can consistently identify and classify nevi that are not visible on US, and enables precise thickness measurement of choroidal nevi, with reduced values compared to US.

KEYWORDS: Choroid; Choroid Neoplasms; Melanoma; Nevus, Pigmented; Tomography, Optical Coherence; Ultrasonography.

RESUMO

INTRODUÇÃO: Analisar a capacidade do *enhanced depth imaging (EDI) - optical coherence tomography* (OCT) de identificar e medir nevus coroideus, e correlacionar os seus achados com características de alto risco.

MÉTODOS: Estudo observacional retrospectivo de doentes com nevus da coróide. Foi feita uma revisão dos registos clínicos e imagiologia multimodal para cada nevus, incluindo EDI-OCT e ultrassonografia (US) modo B. Os indicadores primários foram a espessura da lesão e as suas características na US e EDI-OCT.

RESULTADOS: Foram incluídos um total de 115 *nevus* (106 doentes). Cinco dos 115 *nevus* (4,4%) foram considerados lesões suspeitas. Dos 114 *nevus* com US fidedigna, 83 (72,8%) não foram identificados, comportando-se como *nevus* planos. A média da dimensão basal máxima nos identificados na US foi 5,86 ± 2,19 mm (1,97-10,39 mm), e a média da espessura máxima foi 1,37 ± 0,72 mm (0,45-2,95 mm). Sessenta e dois *nevus* tinham EDI-OCT fidedigno. A média da espessura máxima com EDI-OCT foi 404,93 ± 273,36 μm (139-1504 μm). A espessura máxima medida por US foi significativamente diferente da medida por EDI-OCT (p=0,0011) para cada *nevus*, quando ambos os exames eram fidedignos (US 1233,75 ± 549,57 μm; EDI-OCT 683,19 ± 343,80 μm). Dos 42 *nevus* planos na US que fizeram EDI-OCT sobre a lesão, 38 foram identificados e medidos no EDI-OCT, com uma espessura média inferior ao limiar de deteção da ecografia. Dezoito de 62 *nevus* (29%) tinham elevação na superfície do nevus, e foram classificados como "elevados", tipo 4 no EDI-OCT. O tipo no EDI-OCT foi associado a diminuição da acuidade visual (p=0,014) e a presença de fluido intra ou subretiniano no OCT (p=0,042). As 5 lesões suspeitas foram associadas a características de alto-risco de crescimento ou transformação, como diminuição da acuidade visual, espessura superior a 2 mm, dimensão basal máxima superior a 5 mm e presença de líquido subretiniano.

CONCLUSÃO: O EDI-OCT consegue consistentemente identificar *nevus* coroideus que não são identificados por US, e permite uma medição precisa da sua espessura, com valores mais baixos comparativamente aos obtidos por US.

PALAVRAS-CHAVE: Coróide; Melanoma; Neoplasias da Coróide; Nevo Pigmentado; Tomografia de Coerência Óptica; Ultrassonografia.

INTRODUCTION

The most common benign tumor of the ocular fundus is choroidal nevus. According to The Blue Mountains Eye Study, 6.5% of the adult white population has choroidal nevi.[1] The malignant transformation of choroidal nevi is the main concern of ophthalmologists, as uveal melanoma carries a significant risk of morbidity and mortality. Since nevi are the precursor lesions to many choroidal melanomas, detecting and monitoring choroidal nevi are of supreme importance.

Identification and characterization of choroidal nevi has evolved over the past years from arbitrary ophthalmoscopy labelling of suspicious and non-suspicious nevus, to more objective criteria predictive of transformation. Shields *et al* initially identified as risk factors tumor thickness greater than 2 mm, symptoms of vision loss, floaters and photopsia, presence of subretinal fluid (SRF), presence of orange pigment in ophthalmoscopy, and lesion margin smaller than 3 mm of the optic disc in fundus photography.[2] All these features were essentially determined clinically. Later, surrounding halo and drusen absence, and ultrasonographic hollowness were added,[3] expanding the importance of B-scan ultrasonography (US), but still without the benefit of more advanced imaging. More recently, multimodal imaging has been an extremely helpful tool in ocular oncology, improving tumor diagnosis and understanding. Optical coherence tomography (OCT), fundus autofluorescence (AF) and high-resolution ultrasonography (US) have allowed subclinical detection of subtle features in choroidal lesions such as SRF, intraretinal oedema and orange pigment (lipofuscin), which may not be visible with ophthalmoscopy and fundus photography alone. Shields *et al* analyzed risk factors of choroidal nevi using multimodal imaging for early detection of melanoma, and adjusted the six features that may signify nevi at risk of malignant transformation.[4] Those are thickness greater than 2 mm by US, SRF by OCT, symptoms of visual acuity loss of 20/50 or worse (by Snellen acuity), orange pigment (by AF), melanoma acoustic hollowness (by US) and tumor diameter greater than 5 mm (by fundus photography). Symptoms of flashes/floaters, tumor margin greater than 3 mm to the optic disc, absence of

drusen, and absence of the surrounding halo did not reach significance in the multivariate analysis in that latest study, and are no longer considered risk factors for choroidal nevi.

According to Shields *et al*, thickness greater than 2 mm accounted for the highest hazard ratio in terms of growth and tumor transformation.[4] Therefore, thickness is considered one of the most important features to assess, along with presence of SRF, which accounted for the second highest hazard ratio. As so, accurately measuring choroidal nevi thickness is of utmost importance. Axial and lateral ultrasonography resolution are approximately 100 and 300 μm, respectively. One of the challenges commonly faced in daily practice is assessing and monitoring nevi that cannot be visualized on ultrasonography. Ultrasonographically flat lesions might just represent a choroidal lesion that is thin enough to seem flat on US, carrying difficulties to delineate, measure and consequently, to appropriately follow them up only with B-scan ultrasonography.

Compared to time-domain, spectral-domain OCT (SD-OCT) came with improved sensitivity, speed, and axial resolution, allowing for better detection of retinal and retinal pigment epithelial (RPE) changes secondary to choroidal tumors. However, SD-OCT findings are still limited to the anterior aspect of choroidal nevi, with poor image resolution of structures deep to the RPE, not allowing a full characterization of intrinsic features.[5]

The enhanced depth imaging (EDI) adjustment of SD-OCT brought high-resolution cross sectional imaging of choroidal lesions.[6] Torres *et al* proved that EDI-OCT could objectively measure small choroidal nevi undetectable on US.[7] Jonna *et al* classified ultrasonographically flat lesions into 5 different EDI-OCT patterns, and demonstrated that type 4 nevi ("elevated") denote the higher risk of growth.[8] They also identified SRF as a high-risk feature. It has been proved that EDI-OCT delineates the boundaries of flat nevi with more precision compared with US,[9] but to the best of our knowledge, no study has been made comparing the ability to measure and delineate both flat and non-flat nevi, using EDI-OCT and US.

Knowing that the ability to reliably characterize and follow choroidal lesions over time is crucial for early detection of high-risk changes, a more precise evaluation and measuring technique of choroidal nevi, such as EDI-OCT, might be the next step. We aim to compare EDI-OCT and standard US capacity to measure lesion thickness, and to characterize EDI-OCT features of choroidal nevi.

METHODS

A retrospective observational study was performed, designed to identify all patients who had performed an ultrasonography for choroidal nevi in one or both eyes, at the Ophthalmology Department of Central Lisbon Hospital and Universitary Centre, Lisbon, Portugal, between September 2017 and September 2022. Since the study involved the retrospective collection of anonymized data, ethics approval was waived.

Clinical records, including a complete eye examination with dilated fundoscopy, fundus photography, B-scan ultrasonography (Aviso S, Quantel Medical™, Paris, France), SD-OCT and EDI SD-OCT using the Heidelberg Spectralis system (Heidelberg Engineering, Heidelberg, Germany) and fundus autofluorescence were analyzed. EDI was performed using a technique comparable to that described by Spaide *et al*.[6] Exclusion criteria included: those with chorio-retinal lesions not suggestive of choroidal nevi, lesions suggestive of choroidal melanoma and pigmented lesions suggestive of choroidal melanocytosis.

Demographic characteristics including age, sex, skin color, reason that motivated the ophthalmology appointment, neoplastic known history, age at diagnosis, follow-up duration and interval, and the presence of significant decrease in visual acuity (loss of 20/50 in Snellen or half of the baseline visual acuity) were recorded. The number of choroidal nevi, laterality of eye involved, clinical appearance, findings of multimodal imaging and any change in appearance were also recorded. Specifically, the clinical features recorded included degree of pigmentation (pigmented, nonpigmented), location of the epicentre of the nevus (superotemporal, inferotemporal, superonasal, inferonasal, macular), distance to the optic disc margin (in disc-diameters), shape (round, oval, irregular), largest basal diameter (in disc-diameters), presence of surrounding halo, presence of drusen and presence of orange pigment (lipofuscin). AF features included whether the lesion was visible or not.

B-scan ultrasonography for each nevus was analyzed and two groups were created whether the nevus was identified on B-scan or not, behaving as a flat nevus. The nevi were longitudinally and transversely measured, and the largest basal dimension and its perpendicular basal dimension, nevi maximal thickness and hollow echogenicity were recorded.

EDI SD-OCT characteristics were recorded, including lesion thickness, the presence of drusen, presence of subretinal fluid or intra-retinal fluid and posterior shadowing. Lesion thickness was measured with calipers, with a method equivalent to the one described by Shah *et al*.[9] Lesion thickness including choroid was measured from the sclerochoroidal junction to the outermost boundary or base of the RPE. Lesions were classified into one of 5 groups based on EDI-OCT appearance, as described by Jonna *et al*.[8] All imaging was interpreted, graded and confirmed by two independent reviewers, and in cases of disagreement by a senior retina specialist.

The nevi characteristics and thickness recorded by EDI SD-OCT and B-scan ultrasonography were compared, for each nevus, when both exams were reliable. Patients for whom an OCT exam was not available, mainly due to the peripheral nature of the lesion, were excluded.

Demographics and clinical characteristics were described by frequencies (percentages) and means (standard deviation). Pearson chi-square, Wilcoxon matched-pairs signed-rank test and ANOVA were used when appropriate. A p value <0.05 was considered statistically significant. Data

were analyzed using Statistical Package for the Social Sciences (SPSS) software version 16.0 (SPSS, Inc., Chicago, USA).

RESULTS

One hundred fifteen choroidal nevi in 106 patients (71 women, 45 men) were identified. The mean patient age at nevus diagnosis was 70.9 ± 11.7 years (range 26-95 years). One hundred and two patients (96.2%) were Caucasian and 4 non-Caucasian (3.8%). The mean follow-up length was 4.49±4.69 years (0.5-23 years). The reason that motivated the ophthalmology appointment preceding nevus diagnosis included cataract management (20.9%), diabetic retinopathy screening (17.4%) and glaucoma (10.4%). One patient was referred for having a contralateral melanocytoma, one for having contralateral oculodermal melanocytosis and cutaneous melanoma, one for having a contralateral iris nevus, and one for having a palpebral nevus. Demographic features are detailed in Table 1.

Table 1. Demographic characteristics of patients.

Age at diagnosis, years	70.92 ± 11.68 (26-95)
Gender, n(%)	
Male	35 (33)
Female	71 (67)
Race, n(%)	
Caucasian	102 (96.2)
Non-caucasian	4 (3.8)
Eye n(%)	
Right	60 (52.2)
Left	55 (47.8)
Follow-up time, years	4.49 ± 4.69 (0.5-23)
Nevus number/patient	
One, n(%)	99 (93.4)
Two, n(%)	5 (4.7)
Three, n(%)	2 (1.9)

All the 115 nevi were pigmented nevi. The mean and median number of nevi was 1 (range 1-3). Five (4.4%) of the 115 nevi were considered suspicious lesions by the referring ophthalmologist. The imagiological follow-up interval ranged from monthly to annually. Clinical features are detailed in Table 2.

Of the 115 nevi, 114 (99.1%) had reliable B-scan ultrasonography. Eighty three nevi (72.8%) were not identified, behaving as flat nevi on ultrasonography, and 31 nevi (27.2%) were identified. For the identified nevi, the mean largest basal dimension measured was 5.86 ± 2.19 mm (1.97-10.39 mm). The mean maximal thickness on ultrasonography was 1.37 ± 0.72 mm (0.45-2.95 mm). Seven nevi (6.1%) had hollow echogenicity.

Of the 115 nevi, 93 (80.9%) had reliable OCT performed. Sixty-two of those nevi (66.7%), had reliable EDI-OCT performed. Thirty-one of the 93 nevi did not have EDI-OCT of the nevus available for review, most times because imaging did not capture the nevus due to its far peripheral location.

Table 2. Clinical features of 115 choroidal nevi

Visual acuity decrease n (%)	
Yes	7 (6.6)
No	99 (93.4)
Location n (%)	
Macular	1 (0.9)
Infero-nasal	20 (17.4)
Supero-nasal	12 (10.4)
Infero-temporal	48 (41.7)
Supero-temporal	34 (29.6)
Shape n (%)	
Irregular	42 (36.8)
Oval	31 (27.3)
Round	41 (36.0)
Drusen n (%)	
Present	48 (42.1)
Absent	66 (57.9)
Orange Pigment n (%)	
Present	17 (14.9)
Absent	97 (85.1)
Halo n (%)	
Present	16 (14.2)
Absent	97 (85.9)
Subretinal Fluid n (%)	
Present	32 (28.1)
Absent	82 (71.9)
Papillary margin distance (DD) n (%)	
0	6 (5.3)
> 0 and ≤ 1	18 (15.8)
> 1 and ≤ 2	38 (33.3)
> 2 and ≤ 3	25 (21.9)
> 3 and ≤ 4	22 (21.9)
> 4	4 (4.4)
Mean largest dimension, DD	2.01 ± 1.53 (0.25 – 10.00)

Based on EDI-OCT findings, each choroidal lesion was classified into one of the distinct OCT patterns: 5 of 62 nevi (8.1%) were not visible on EDI-OCT imaging (classified as type 0); 28 of 62 nevi (45.2%) demonstrated hyperreflectivity confined within normal choroidal thickness (type 1); 8 of 62 nevi (12.9%) had anteriorly bowed hyperreflectivity cascading at discrete lesion edges with dark posterior shadowing (classified as "discrete", type 2); 3 of 62 nevi (4.8%) had a flat surface but with a "posterior bowing" with scleral excavation (classified as type 3); and 18 of 62 nevi (29%) had elevation of the surface of the nevus (classified as "elevated",

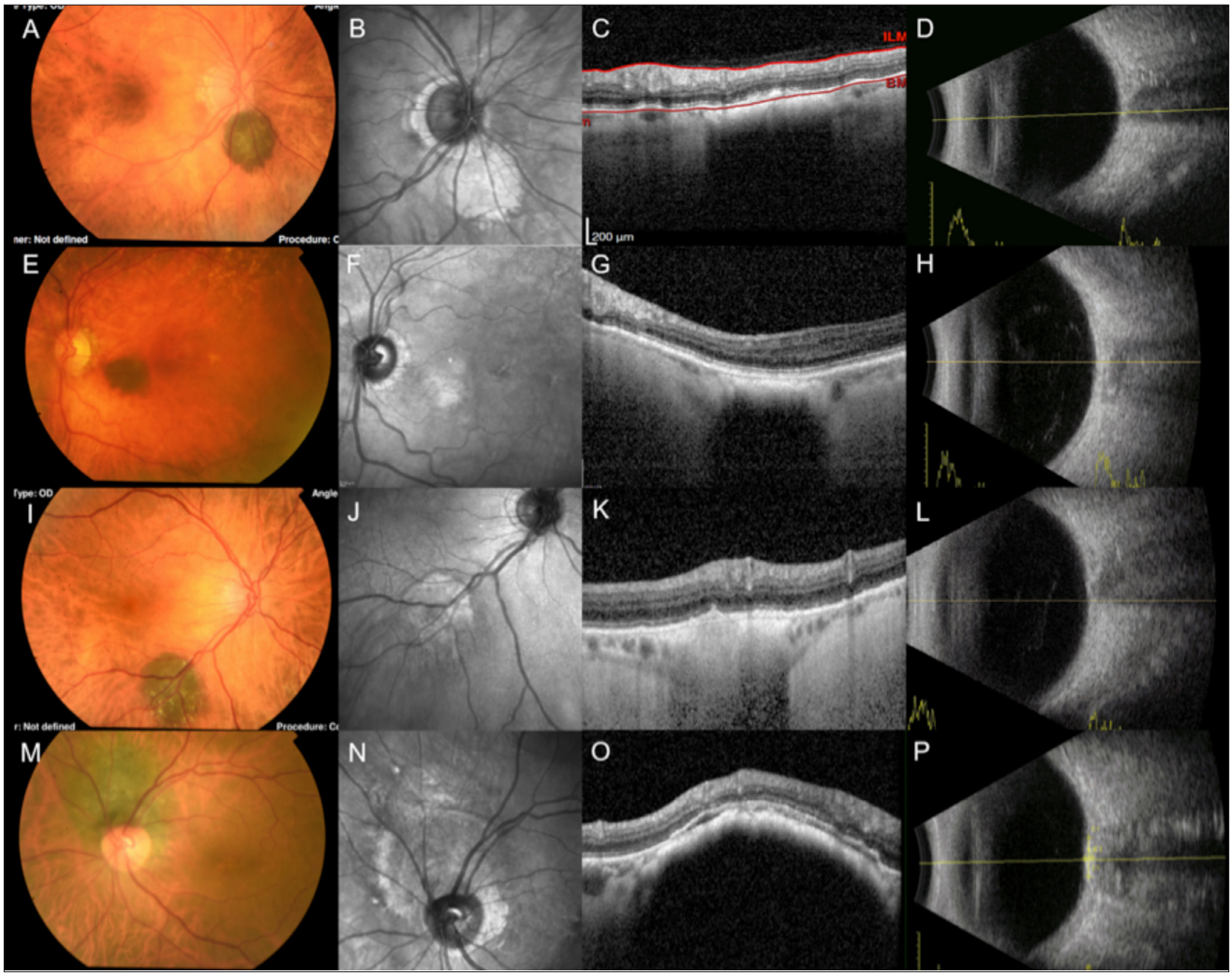

Figure 1. Enhanced depth imaging (EDI) – OCT Type 1-4 and multimodal imaging of choroidal nevi.
A-D, Type 1 "hyperreflective" lesion. A – pigmented lesion without drusen or orange pigment; B – the lesion seems white on infrared (IR); C – the lesion is hyperreflective but confined within normal choroidal thickness on EDI-OCT; D – flat appearance on US; E-H, Type 2 "discrete" lesion. E – pigmented nevus without drusen or orange pigment; F – the lesion seems pale on IR; G – the lesion seems discrete (anteriorly bowed hyperreflectivity cascading at lesion edges) on EDI-OCT; H – flat appearance on US; I-L, Type 3 "posteriorly bowed" lesion. I – pigmented nevus with drusen but no orange pigment; J – the lesion seems pale on IR; K – the lesion looks posteriorly bowed on EDI-OCT; L – flat appearance on US; M-P, Type 4 "elevated" lesion. M – pigmented lesion without drusen or orange pigment; N – the lesion is darker on IR; O – elevated lesion on EDI-OCT; P – peripapillary lesion with high anterior reflectivity with 4 mm of largest basal dimension and 1.2 mm of thickness on US.

type 4). OCT features and patterns are detailed in Table 2. Fig. 1 shows representative fundus photos and EDI-OCTs of the 5 different subtypes. Two of the 62 nevi (3.2%) were thicker than the EDI-OCT scans, so their thickness could not be measured. For the 60 measurable nevi, mean maximum thickness was 404.93 ± 273.36 µm (139-1504 µm). The relationship between EDI-OCT types and clinical characteristics of the choroidal lesions is detailed in Table 3.

The relationship between B-scan ultrasonography and EDI-OCT findings for each nevus, in cases where both exams were reliable, are detailed in Table 4. The nevi maximum thickness measured in B-scan ultrasonography was significantly different from the maximum thickness measured by EDI-OCT (p=0.0011), for the same nevus. The mean maximum thickness measured by US was 1233.75 ± 549.57 µm (450-2400 µm), while the mean maximum thickness measured in EDI-OCT was 683.19 ± 343.80 µm (255-1504 µm). Thirty-eight of the 42 flat nevi on US that had an EDI-OCT performed over the lesion, were identified and measured in EDI-OCT. Their mean thickness in EDI-OCT was 289.95±117.87 µm (139-696 µm).

The mean largest basal dimension in ultrasonography was not correlated with OCT type (p=0.145). Twelve of the 17 nevi (70.6%) measured both by US and OCT were classified as OCT-type 4.

All the 5 OCT-type 0 lesions were flat lesions on US. Three of the 28 OCT-type 1 lesions (10.7%) and 3 of the 8 OCT-type 2 lesions (37.5%) were identified on US. Of the 3

Table 3. Enhanced Depth Imaging OCT features of choroidal nevi	
Mean choroidal lesion thickness, μm	404.93 ± 273.36 (N=55 measurable)
EDI SD-OCT Pattern n (%)	N = 62
Type 0 = Not visible	5 (8.1)
Type 1 = Hyperreflective but confined within normal choroidal thickness	28 (45.2)
Type 2 = Discrete (waterfall appearance at lesion edges)	8 (12.9)
Type 3 = Posteriorly bowed	3 (4.8)
Type 4 = Elevated	18 (29)
Posterior shadowing n (%)	
Present	45 (72.6)
Absent	17 (27.4)
Drusen n (%)	
Present	20 (32.3)
Absent	42 (67.7)
Sub/intraretinal fluid n (%)	
Present	10 (16.1)
Absent	52 (83.9)

OCT-type 3 lesions, none (0%) was identified on US. Of the 18 EDI-OCT type 4 lesions, 13 (72.2%) were identified on US. The mean EDI-OCT thickness of the 5 non-identified on US type 4 nevi was 449.40±178.41 μm (257-696 μm).

EDI-OCT type was positively associated with the presence of decrease in visual acuity to more than half of the previous visual acuity (p=0.014). Six of the 7 nevi (85.7%) with decrease in visual acuity were classified as EDI-OCT type 4. There was a significant association between EDI-OCT type and the presence of intra-retinal fluid (IRF) or sub retinal fluid (SRF) on OCT (p=0.042). Seven of the 10 nevi (70%) with IRF/SRF were classified as EDI-OCT type 4. There was an association between EDI-OCT type and the presence of shadowing in OCT (p<0.001). Forty-five of the 60 nevi (75%) had shadowing in OCT.

There was no significant association between EDI-OCT type and nevi location (p=0.195), nevi shape (p=0.974) and nevi largest dimension on US (p=0.145). The presence of orange pigment (p=0.393), the presence of drusen (p=0.219) and the presence of surrounding halo (p=0.361) was not associated with EDI-OCT type.

Of the 5 suspicious lesions, 1 had no reliable EDI-OCT available. The other 4 belonged to the EDI-OCT type 4. All the 5 lesions had US thickness of more than 2 mm, with

Table 4. EDI-OCT findings correlated with known high-risk features.

EDI-OCT Type	Visual acuity decrease (%)	Mean Diameter in Fundus photography (DD)	Orange pigment by AF (%)	Subretinal fluid in OCT (%)	US Hollow n (%)	Mean US thickness (mm)	Mean OCT thickness (μm)
0	0	0.75	0	0	0	-	0
1	3.8	1.82	14.3	7.1	3.6	1.12	263.71
2	0	2.13	25.0	12.5	12.5	0.92	359.00
3	0	2.0	33.3	0	0	-	276.33
4	35.3	2.92	33.3	38.9	16.7	1.56	699.13

Table 5. High risk features of suspicious lesions.

Suspicious Lesions	EDI-OCT Type	LBD (mm)	US thickness (mm)	OCT thickness (μm)	Visual acuity decrease	Orange pigment	Subretinal fluid	US Hollow
1	4	4.68	2.03	683	Yes	Yes	Yes	No
2 (far peripheral lesion)	-	9.11	2.95	-	No	No	No	Yes
3	4	9.69	2.95	0	Yes	Yes	Yes	Yes
4	4	8.27	2.4	797	Yes	Yes	Yes	No
5	4	6.71	2.72	-	Yes	No	No	No

lower values obtained with EDI-OCT. Two of those lesions were too large to be measured with the OCT scans. Four had the largest basal dimension greater than 5 mm, four had a decrease in visual acuity of 20/50 or more. Three had SRF, three had orange pigment and 2 had US hollow. The EDI-OCT, B-scan US and the clinical risk features of the 5 suspicious choroidal lesions are detailed in Table 5.

DISCUSSION

This study included 115 pigmented nevi. One hundred-fourteen (99.1%) had reliable B-scan US, however, only 31 nevi (27.2%) were identified on US. The remaining 83 nevi (72.8%) were classified as flat lesions. Although US has long been used to detect choroidal nevi, it lacks sensitivity, es-

pecially for smaller lesions. It has been demonstrated that choroidal tumors with thickness smaller than 1 mm, undetectable by US, could be detected and measured with EDI-OCT.[7] In this study, ninety percent of flat nevi on US were successfully identified and measured in EDI-OCT, with a mean thickness of 289.95±117.87 μm.

One of the main established risk factors for nevus growth is tumor thickness greater than 2 mm.[2–4] Accurately measuring choroidal lesions is of utmost importance. US has been previously shown to lack consistency, and to overestimate choroidal melanoma thickness.[9,10] In agreement, the mean maximal thickness of choroidal nevi measured by US in this study, was greater than the one measured by EDI-OCT (1233.75 ± 549.57 μm, 683.19 ± 343.80 μm, respectively). It may be explained by inadvertently including retinal and, at times, scleral thickness in the US thickness measurement, making it less reliable than EDI- OCT.

EDI-OCT can identify features beyond the anterior surface of the nevus and delineate its borders, including the posterior one.[7] Sixty-two nevi had reliable EDI-OCT performed over the lesion. The classification system into 5 distinct EDI-OCT patterns suggested by Jonna *et al*, was applied.[8] Type 0 lesions are believed to correspond to focal hyperpigmentation of histologically normal choroid, with no nevus cells. Type 1 lesions are thought to represent replacement of at least part of the choroid with nevus cells, what may be called the choroidal ephelis.[11] Type 2 lesions are believed to be conditioned by imaging artefacts, as the nevi cell spindle shape and orientation increase reflectivity. Type 3 nevi are believed to represent real nevi that appear flat at the surface, since the expansion extends posteriorly into the sclera, causing excavation. Type 4 nevi are also considered true nevi with measurable height. In these lesions, there is not typically an anterior hyperreflectivity causing a posterior shadowing, so their thickness can be more accurately measured.

Of the 18 EDI-OCT type 4 lesions in our study, 13 (72.2%) were identified on US. Five nevi (27.8%) were not identified and consequently not measured by US. That may have happened because the nevi height could be below the US detectability threshold. Knowing that type 4 nevi are at a higher risk of growth or transformation,[8] it is critical to identify all these lesions, and to measure them. As US resolution and detectability threshold is inferior to EDI-OCT, we consider that EDI-OCT should be performed for all the nevi.

Focusing on the 6 risk features highlighted by Shields *et al*, we may notice that thicker nevi and SRF/IRF were more frequently found on EDI-OCT type 4. Similarly, visual acuity loss of 20/50 or worse was mainly found on EDI-OCT type 4 lesions. Six of 7 nevi with decrease in visual acuity belong to that group, which could be easily understood taking into consideration the fact that the type 4 lesions present with elevation of the nevus surface, with possible distortion of the adjacent retinal layers. In our study, orange pigment was not associated with EDI-OCT type, probably influenced by the absence of AF imaging in some patients. Largest basal dimension was also not associated with EDI-OCT type, which is easily understood since EDI-OCT classification does not take into consideration the longitudinal and transversal dimension, but the nevi and surrounding structures' morphological features. The cut-off basal dimension value established of greater than 5 mm did not represent a distinctive feature as a risk factor since the mean diameter of our sample was greater than 5 mm. Despite not statistically significant, 3 of the 5 nevi presenting with ultrasonographic acoustic hollowness (with reliable EDI-OCT) belonged to EDI-OCT type 4.

Corroborating previous studies,[3,4,9] distance to the optic disc margin, presence of drusen and presence of surrounding halo, nevus location and shape were not correlated to EDI-OCT type.

Of the 5 lesions considered suspicious of melanoma progression in our study, 1 was located on the far periphery with no reliable EDI-OCT available, and the other 4 belonged to the EDI-OCT type 4. High-risk features of lesion growth or transformation, such as thickness of more than 2 mm by US, largest basal dimension greater than 5 mm, orange pigment and hollow US were commonly found in these lesions. Thus, it is imperative to tightly monitor these nevi, with a multimodal imaging follow-up.

The strengths of our study included good sample size, comprehensive and consistent clinical examination, and regular imaging protocol. The limitations of our study included a retrospective design, variable follow-up, and inability to image with EDI-OCT a fraction of choroidal lesions, that occurred most of times in the far periphery. A prospective study with standardized imaging of choroidal nevi with B-scan US and EDI-OCT would be interesting to compare over time their capacity to identify and measure choroidal lesions, and to evaluate possible growth or change. Although our sample size is similar to other published studies, given the low diagnosis and growth rate of these lesions, larger studies are recommended.

CONCLUSION

Knowing that nevi can be melanoma precursor lesions, it is vital to detect and monitor these lesions. Our study corroborated EDI-OCT's ability to consistently identify choroidal nevi, even in cases where US could not. High-risk features predictive of growth and transformation have been defined, to help signify lesions that may require a closer follow-up. EDI-OCT provides a better visualization and delineation of the posterior limits of choroidal tissue, allowing for more accurate and precise measurements of nevi thickness, compared to US. EDI-OCT successfully identified other risk features such as the presence of SRF. The EDI-OCT classification based on nevus phenotype and the surrounding structures' morphology could add some value to the nevus risk stratification, since EDI-OCT type 4, "elevated" lesions, tended to be associated with other known high-risk features such as decrease in visual acuity, presence of SRF and thickness greater than 2 mm.

With the EDI-OCT ability to reliably identify and accurately measure nevi thickness, choroidal lesions can be monitored objectively, with the aim of early detection of lesions that may grow and undergo malignant transformation. A comprehensive assessment and monitoring of every

choroidal nevus is required, including a clinical observation and multimodal imaging. To the established importance of clinical ophthalmoscopy, fundus photography, Snellen chart, US, OCT and AF, we suggest adding EDI-OCT, not only to classify and identify flat lesions on US but also to measure ultrasonographically identified nevi.

CONTRIBUTORSHIP STATEMENT / DECLARAÇÃO DE CONTRIBUIÇÃO:

BC: Responsible for gathering the data, presenting the results, and creating the manuscript.

PG, DHF: Responsible for the statistical analysis and the manuscript revision.

CM: Contributed for the data collection.

AM: Supervised this project and contributed with her expertise to its conclusion.

All the authors read and approved the final manuscript. All the authors had full access to all the data and take full responsibility for the integrity of the data and the accuracy of the data analysis; all were responsible for conceiving this research.

RESPONSABILIDADES ÉTICAS

Conflitos de Interesse: Os autores declaram a inexistência de conflitos de interesse na realização do presente trabalho.

Fontes de Financiamento: Não existiram fontes externas de financiamento para a realização deste artigo.

Confidencialidade dos Dados: Os autores declaram ter seguido os protocolos da sua instituição acerca da publicação dos dados de doentes.

Proteção de Pessoas e Animais: Os autores declaram que os procedimentos seguidos estavam de acordo com os regulamentos estabelecidos pela Comissão de Ética responsável e de acordo com a Declaração de Helsínquia revista em 2013 e da Associação Médica Mundial.

Proveniência e Revisão por Pares: Não comissionado; revisão externa por pares.

ETHICAL DISCLOSURES

Conflicts of Interest: The authors have no conflicts of interest to declare.

Financing Support: This work has not received any contribution, grant or scholarship

Confidentiality of Data: The authors declare that they have followed the protocols of their work center on the publication of data from patients.

Protection of Human and Animal Subjects: The authors declare that the procedures followed were in accordance with the regulations of the relevant clinical research ethics committee and with those of the Code of Ethics of the World Medical Association (Declaration of Helsinki as revised in 2013).

Provenance and Peer Review: Not commissioned; externally peer reviewed.

REFERENCES

1. Sumich P, Mitchell P, Wang JJ. Choroidal nevi in a white population: the Blue Mountains Eye Study. Arch Ophthalmol. 1998;116:645-50. doi: 10.1001/archopht.116.5.645.
2. Shields CL, Mashayekhi A, Materin MA, Luo CK, Marr BP, Demirci H et al. Optical coherence tomography of choroidal nevus in 120 patients. Retina. 2005;25:243-52. doi: 10.1097/00006982-200504000-00001.
3. Shields CL, Furuta M, Berman EL, Zahler JD, Hoberman DM, Dinh DH, et al. Choroidal nevus transformation into melanoma: analysis of 2514 consecutive cases. Arch Ophthalmol. 2009;127:981-7. doi: 10.1001/archophthalmol.2009.151.
4. Shields CL, Dalvin LA, Ancona-Lezama D, Yu MD, Nicola MD, Williams Jr BK, et al. Choroidal nevus imaging features in 3,806 cases and risk factors for transformation into melanoma in 2,355 cases. Retina. 2019;39:1840-1. doi: 10.1097/IAE.0000000000002440.
5. Sayanagi K, Pelayes DE, Kaiser PK, Singh AD. 3D spectral domain optical coherence tomography findings in choroidal tumors. Eur J Ophthalmol. 2011;21:271-5. doi: 10.5301/EJO.2010.5848.
6. Spaide RF, Koizumi H, Pozonni MC. Enhanced depth imaging spectral-domain optical coherence tomography. Am J Ophthalmol. 2008;146:496-500. doi: 10.1136/bjophthalmol-2020-318095.
7. Torres VLL, Brugnoni N, Kaiser PK, Singh AD. Optical coherence tomography enhanced depth imaging of choroidal tumors. Am J Ophthalmol. 2011;151:586-593.e2. doi: 10.1016/j.ajo.2010.09.028.
8. Jonna G, Daniels AB. Enhanced depth imaging OCT of ultrasonographically flat choroidal nevi demonstrates 5 distinct patterns. Ophthalmol Retin. 2019;3:270-7. doi: 10.1016/j.oret.2018.10.004.
9. Shah SU, Kaliki S, Shields CL, Ferenczy SR, Harmon SA, Shields JA. Enhanced depth imaging optical coherence tomography of choroidal nevus in 104 cases. Ophthalmology. 2012;119:1066-72. doi: 10.1016/j.ophtha.2011.11.001.
10. Collaborative Ocular Melanoma Study Group. Comparison of Clinical, Echographic, and Histopathological Measurements From Eyes With Medium-Sized Choroidal Melanoma in the Collaborative Ocular Melanoma Study. Arch Ophthalmol. 2003;121:1163-71. doi: 10.1001/archopht.121.8.1163.
11. Shields, Jerry A. and CLS. Intraocular Tumors: An Atlas and Textbook. Berlin: Lippincott Williams & Wilkins; 2008.

Corresponding Author/
Autor Correspondente:

Bruna Cunha
Alameda Santo António dos Capuchos,
1169-050 Lisboa, Portugal
E-mail: bruna_cunha_44@hotmail.com

ORCID: 0000-0002-1273-1893